

## Crosstalk Improvement of Polymer in Glass Thermo-Optical Multimode Interference Switch

N. Samdin, M. Yaacob, M.H. Ibrahim\*, A.B. Mohammad, N.M. Kassim

Lightwave Communication Research Group, Infocomm Research Alliance, Universiti Teknologi Malaysia  
81310 Skudai, Johor, MALAYSIA  
e-mail: hanif@fke.utm.my\*

### Abstrak

Sebuah desain struktural baru yang menggabungkan atenuator optik variabel (VOA) dan saklar optik diusulkan dalam makalah ini. Desain didasarkan pada arsitektur interferensi multimode (MMI) dan desain ini telah menunjukkan peningkatan crosstalk saklar optik. Perangkat beroperasi dengan memanipulasi efek optik-termo (TO) yang secara alami ada di semua materi pemandu-gelombang optik. Dengan menerapkan suatu polimer pada platform material kaca, VOA dioptimalkan dengan pelemahan optik 21,52 dB telah dicapai dengan daya 36,4 mW. Hasil simulasi menunjukkan bahwa VOA membantu untuk mencapai perbaikan yang signifikan kinerja saklar optik khususnya di pengurangan crosstalk hingga 89,66%.

**Keywords:** atenuator optik variabel, crosstalk, interferensi multimode, optik-termo, saklar optik

### Abstract

A new structural design of combined variable optical attenuator (VOA) and optical switch has been proposed in this paper. The design is based on the multimode interference (MMI) architecture and it has been demonstrated for crosstalk improvement of optical switch. The device operates by manipulating thermo-optic (TO) effect that naturally existed in all optical waveguide material. By applying a polymer on glass material platform, the optimized VOA with optical attenuation of 21.52 dB has been achieved with applied power of 36.4 mW. The simulation result shows that the VOA helps to achieve significant improvements of optical switch performance particularly in crosstalk reduction up to 89.66%.

**Keywords:** crosstalk, multimode interference, optical switch, thermo-optic, variable optical attenuator

### 1. Introduction

High speed and high capacity optical components are crucially needed in current optical networks. For this, it is very necessary to research for good and tolerable performances of optical switch. Furthermore, it is important to develop optical devices with low power consumption and crosstalk. Interestingly, multimode interference (MMI) structure is a good candidate for these purposes. Although numbers of MMI optical switches have been developed which progressively claimed low switching power results, the crosstalk issue is yet to be solved.

Variable optical attenuator (VOA) is a device that functions to adjust optical power in the optical devices interconnection system. Few types of VOA structure have been developed; for example Mach-Zehnder interferometer (MZI) based VOA [1-3], straight waveguide based VOA [4-6] and multimode interference (MMI) based VOA [7-8]. From the survey on type of developed VOA, it shows that the MMI structure have the smallest power consumption; 7.8mW [8] compared with other type of VOA structure. Obviously, the MMI structure is a good candidate for VOA design.

For MMI-VOA structure, there two types of VOA that have been develop previously which are; a combination of two MMI structure to be operate as MZI-VOA [9] and single MMI-VOA [10]. In the MZI-VOA, the structure is composed of an MMI power splitter with single inputs and re-combined with double output to the other MMI combiner with single output. The active region (induced by electro or thermo effect) is located at the phase shift arms and used to change the relative phases among the arms, which can realize the attenuation function [11]. Concurrently, a single coupler of MMI-VOA is realized through refractive index modulation. The refractive index modulation leads to the variation of the imaging intensity within the MMI region. As a result, the output images can be attenuated which further realize the attenuation function.

Notably, thermo-optic effect is the most popular approach to attain refractive index modulation in heated dielectric material. Thermo-optic coefficient,  $dn/dT$  is an important optical constant related to thermo-optic effect. Typically, for polymer  $dn/dT \sim -10^{-4}/^{\circ}\text{C}$  while for silica  $dn/dT \sim 10^{-5}/^{\circ}\text{C}$ . As polymer is having a high  $dn/dT$  which is 10 times higher than silica, it can be concluded that index modulation of polymer are more dependent on the temperature or easy to actively control. Thus it takes less power to induce thermo-optically in polymer waveguide compared to silica waveguide [12]. In addition, polymeric materials are particularly attractive in integrated optics because of their ability to be processed rapidly, cost-effectively, and with high yields [13-14]. Based on our previous work on photodefinable BenzoCyclobutene (BCB 4024-40) polymer in optical devices development [15-17], we have successfully demonstrates that BCB 4024-40 polymer is a suitable material to be adopted in our future works on optical switches and attenuators.

In order to reduce the crosstalk figure, we propose a new structural design of polymer in glass optical switch structure consists of 2x2 thermo-optic MMI switch and two single couplers MMI-VOA, with both elements integrated in series. Finite difference beam propagation method (FD-BPM) is employed in this work to simulate the performance of proposed design. It is shown that the integration of MMI-VOA gives significant improvement in crosstalk performance compared with those of a conventional MMI optical switch.

## 2. Operation Principle and Device Structure

The property of MMI coupler is based on the principal of the self-imaging effect [18-19]. The principal can be stated as the input is reproduced in single or multiple images at periodic intervals along the propagation direction of the guide [20]. Two types of self-imaging mechanism has been discussed in detail by Soldano and Pennings [20] known as general interference (GI) and restricted interference (RI). In RI, the MMI device can be designed either by paired or symmetric interference MMIs depending on the field excitation condition. Due to the mode excitation in MMI section, the interference among these modes will produce single or multiple self image of the input field at certain distance. In general interference, single images of the input field can be attained at

$$L = p (3L_{\pi}) \quad \text{with} \quad p = 0, 1, 2, 3, \dots \quad (1)$$

Here,  $p$  refers to the periodic number of the imaging along the multimode waveguide.  $L_{\pi}$  is defined as the beat length of the two lowest order modes and can be written as:

$$L_{\pi} = \frac{\Pi}{(\beta_0 - \beta_1)} \quad (2)$$

where  $\beta_0$  and  $\beta_1$  are the propagation constant of the fundamental and first order modes, respectively. For paired interference, the direct and mirrored single images of the input field will be formed at the multimode section length of:

$$L = p(L_{\pi}) \quad (3)$$

The direct and mirrored single images correspond to bar and cross coupling state, respectively.

## 3. Design of Thermo-Optic Multimode Interference Switch

The basic architecture of optical switch is designed according to the 2x2 MMI based cross coupler. Polymer in silica has been applied in designing the 2x2 MMI based cross coupler. The MMI coupler consists of BenzoCyclobutene (BCB 4024-40) polymer ( $n_2=1.5556$ ) [21] as core layer surrounded by BK7 lower clad ( $n_3=1.5010$ ) [22] and silica ( $\text{SiO}_2$ ) upper clad ( $n_1=1.45$ ) [23].

In our design, the switch structure was layered by deposition of  $4\mu\text{m}$  thick of core,  $6\mu\text{m}$  thick of upper clad and  $20\mu\text{m}$  thick of lower clad. A silicon wafer was used as substrate layer and  $2000\text{ \AA}$ -thick aurum was shaped as a straight heater on top of upper clad layer. In addition, sufficient distance between heater electrode and waveguide are needed to avoid any loss due to lossy metal behavior [23]. Meanwhile, the lower clad is bound to attenuation into Si substrate [24]. Figure 1 shows the cross section of the thermo-optic MMI switch with a straight heating electrode.

The basic configuration of the MMI coupler was designed according to the paired interference mechanism. For paired interference scheme, the input access waveguide have to be placed at  $1/3$  or  $2/3$  of the MMI section width [20]. Two single mode access waveguide enter the MMI region with dimension of  $4\times 4\mu\text{m}^2$ . A schematic view of designed thermo-optic MMI switch is illustrated in Figure 2. The heater is optimized to be  $6\mu\text{m}$  wide and  $3508\mu\text{m}$  long, corresponding to the length of MMI coupler. In addition, the heater electrode is positioned  $20\mu\text{m}$  right to the symmetry axis. Detail optimization of thermo-optic MMI switch parameter can be found in our previous publication [25].

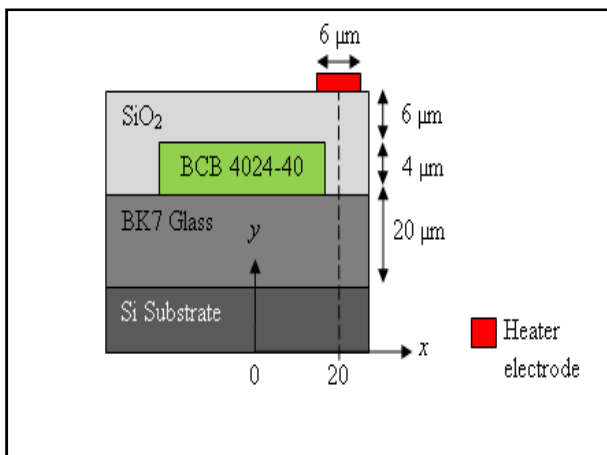


Figure 1. Cross section of the thermo-optic MMI switch with a straight heating electrode

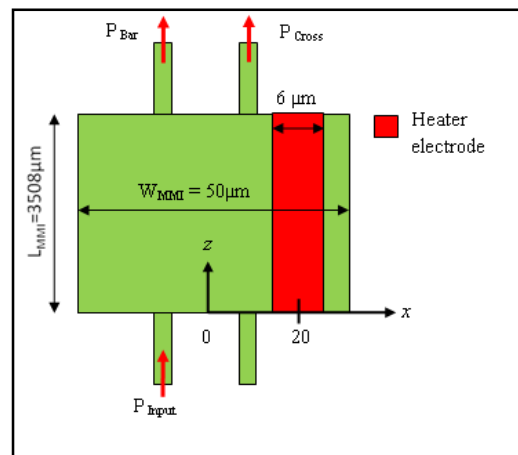


Figure 2. Schematic configuration of the thermo-optic MMI switch with a straight heating electrode

Polymer material has been regarded as one of the main materials that exhibit the thermo-optic (TO) effect that can be further manipulated to be applied in the development of thermo-optic switch. This is due to the significant advantages offered by this material such as low thermal conductivity and greater temperature dependence of refractive index [12]. The essential thermal properties of material are listed in Table 1.

Table 1. Thermal properties

Material	Thermal Conductivity, (W/m.K)	Thermal Coefficient, $dn/dT$
BCB 4024-40 Polymer [21]	0.29	$-1.5 \times 10^{-4}/K$
BK7 Glass [22]	1.114	$1.1 \times 10^{-6}/K$
SiO <sub>2</sub> [23]	1.4	$8 \times 10^{-6}/K$
Silicon Substrate	163.3	$160 \times 10^{-6}/^{\circ}C$

The simulation was done by employing BeamProp™ software from RSoft™ and shown in Figure 3. Without thermal tuning, the structure operates like normal cross coupler. Therefore, light will emit at output port  $P_{\text{Cross}}$  when input light at the wavelength of  $1550\text{nm}$  is fed from input port  $P_{\text{Input}}$  as shown in Figure 3(a). However, as electric power is applied to the electrode heater, the refractive index beneath the electrode heater will decrease due to the negative TO coefficient of the polymeric materials. Consequently, major light confinement will shift to the output port  $P_{\text{Bar}}$  as the light propagation always at high refractive index region. Thus, optical

switching can be achieved. Figure 3(a) and (b) shows the optical power distribution in which no heat is applied and the heater is powered, respectively. Temperature distribution plot for straight heater analysis (power applied =54.41mW) is shown in Figure 4. Maximum temperature rise induced by heater electrode is around 56° Kelvin.

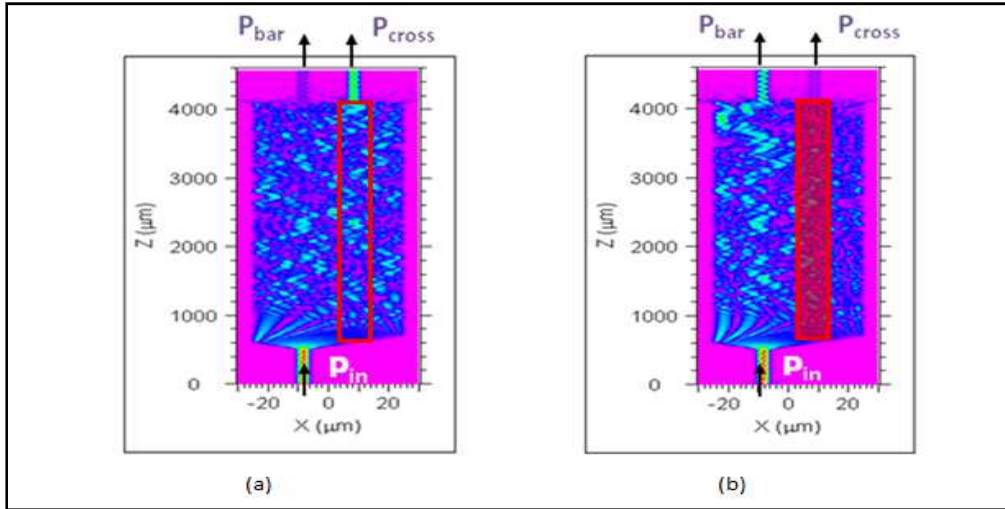


Figure 3. Beam Propagation Method (BPM) analysis of MMI switch for optical power distribution (a) without thermal tuning and (b) with thermal tuning

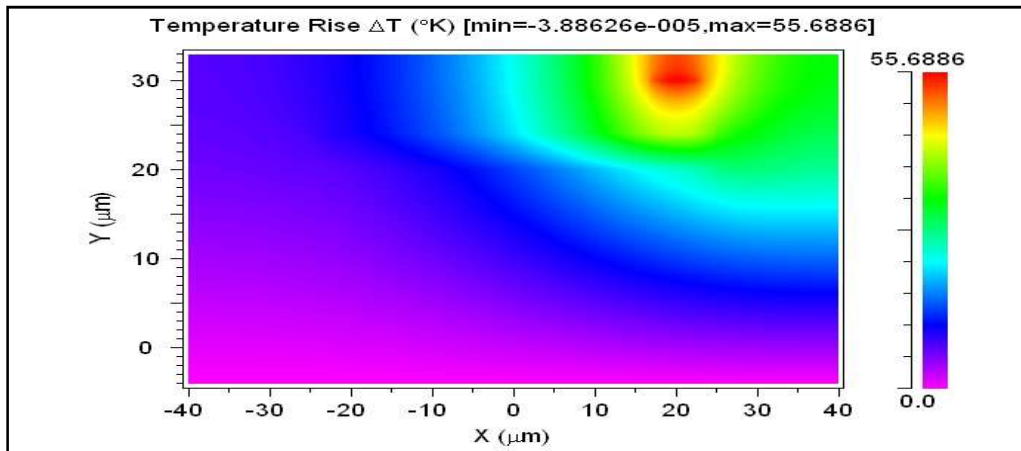


Figure 4. Temperature distribution plot for straight heater analysis when power applied is 54.41mW

Optical switch is mainly characterized by driving power and crosstalk. The driving power needed by heater electrode to change refractive index can be calculated by

$$Power = \frac{\rho L}{wh} I^2 \quad (Watt) \tag{4}$$

where,  $I$  is the current through the heater electrode,  $\rho$  is the resistivity,  $L$  is the length,  $w$  is the width and  $h$  is the thickness of the heater electrode. Aurum has been chosen as suitable material for heater electrode due to its high thermal conductivity of 318 W/m°C [24]. The resistivity,  $\rho$  of Au is  $2.068 \times 10^{-8} \Omega m$ . Crosstalk is defined as the ratio of the power leaked to

the wrong output to the power in the correct output. Therefore, crosstalk for cross state can be expressed as [26]

$$\text{Crosstalk} = 10 \log \frac{P_{out,bar}}{P_{out,cross}} \quad (\text{dB}) \quad (5)$$

Here,  $P_{out,bar}$  is the optical power at the unwanted waveguide and  $P_{out,cross}$  is the output power at the desired waveguide. The switching characteristic for optical switch is represented in Figure 5. Noted that at a driving power of 54.41 mW, switching operation occurred with crosstalk performance of -19.14 dB.

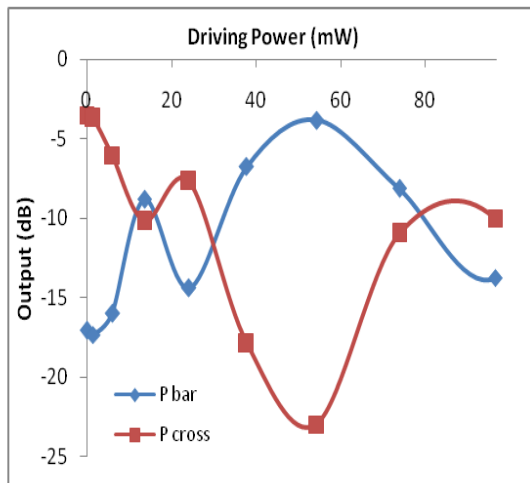


Figure 5. Switching characteristics of the thermo-optic MMI switch with 6 $\mu\text{m}$  of straight heater electrode

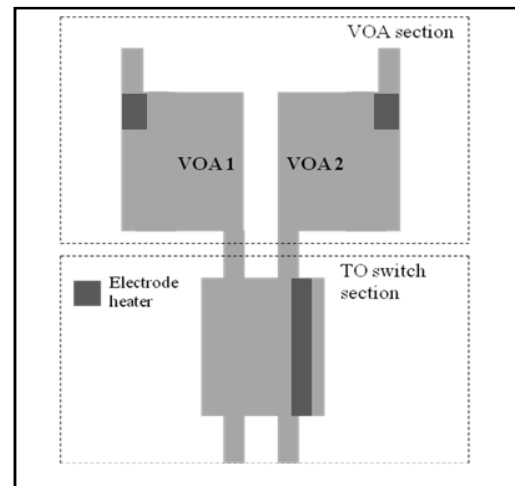


Figure 6. Top view of integrated thermo-optic MMI switch and MMI VOA

#### 4. Design of Multimode Interference Variable Optical Attenuator (VOA)

In this work, MMI structure has been proposed in VOA design by using general interference (GI) mechanism. GI was selected to realize 250 $\mu\text{m}$  standard fiber array separation distance. The MMI-VOA will be integrated with the thermo-optic MMI switch (previously discussed) in order to attenuate the excessive power at unwanted output from thermo-optic MMI switch. The MMI VOA was positioned at both outputs of thermo-optic MMI switch. Figure 6 shows a schematic diagram of the entire proposed device, with the MMI-VOA connected to the thermo-optic MMI switch.

A schematic diagram of the proposed MMI-VOA is shown in figure 7. The structure consists of 50  $\mu\text{m}$  wide and 12147  $\mu\text{m}$  long of MMI section with the heater electrode was placed on the upper clad above the embedded MMI section. The cross section of MMI-VOA is set to be the same design as thermo-optic MMI switch for integration purpose. The heater electrode was optimized to be 6  $\mu\text{m}$  wide and 2347  $\mu\text{m}$  long at 22  $\mu\text{m}$  right from the center of MMI region. Justification for the proposed size and position of heater electrode can be obtained from Samdin's thesis [27].

The operating principle of the attenuator is as follow. When electrical power is applied along the heater electrode, the refractive index under the heated electrode is reduced by negative TO effect of polymeric material. As a result, the imaging intensity under heated electrode region effectively attenuated. Hence, an excessive optical power from unwanted output port from TO switch can be eliminated. The ideal excessive power removal can improve the performance of thermo-optic switch particularly in crosstalk performance. Figure 8 shows the light propagation for proposed MMI-VOA using finite difference beam propagation method (FD-BPM).

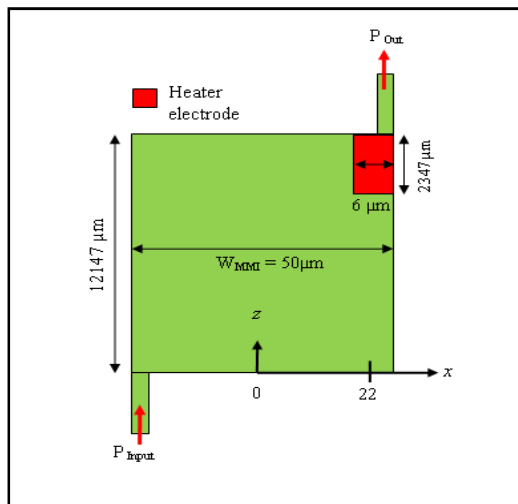


Figure 7. Schematic layout - GI scheme of MMI VOA

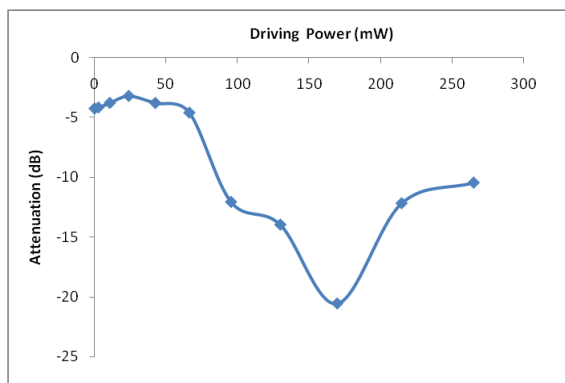


Figure 9. Calculated driving power and attenuation of VOA (heater electrode positioned 22  $\mu\text{m}$  from the center of MMI)

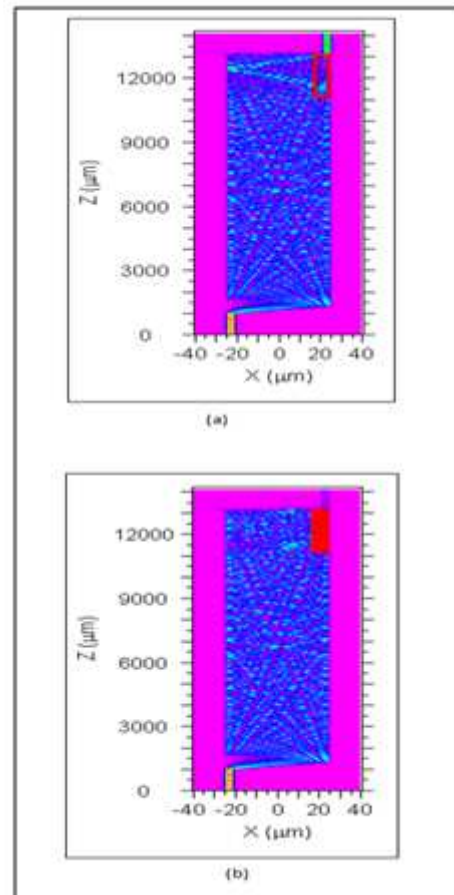


Figure 8. Light propagation for proposed MMI VOA (a) with no power applied (b) with the applied power of 36.4 mW

## 5. Results and Discussion

In the beginning, the emphases have been steered simultaneously towards the optimization of position and the width of the heater electrode. The calculated VOA characteristic for 6  $\mu\text{m}$  wide of heater electrode at position of 22  $\mu\text{m}$  is shown in Figure 9. Noted that high driving power of 169.49 mW is required to attain attenuation level of -20.56 dB. However, equation (3.1) demonstrates that the driving power can be reduced by shortening the length of heater electrode. Hence, further analysis and optimization was carried out for the heater electrode length.

The driving power and attenuation of VOA were calculated for several heater electrode lengths from 147  $\mu\text{m}$  to 6147  $\mu\text{m}$ . From the simulation result, the driving power and attenuation of VOA as a function of heater electrode length has been plotted in graph as presented in Figure 10. As expected, the driving power value decreased with respect to the heater electrode length presented in fluctuating form. The heater electrode length of 2347  $\mu\text{m}$  was selected to simultaneously produce a VOA with low driving power of 36.4 mW and low attenuation level of 21.52 dB.

The attenuation characteristic of optimized VOA in term of position, width and length of heater electrode is illustrated in Figure 11. Simulation was done for the entire devices which include integration of MMI switch and MMI-VOA. It was observed that the total power consumption is 90.81 mW with improved crosstalk level of -36.37 dB. Thus, it indicates the crosstalk improvement up to 89.66% when the MMI TO switch is integrated with MMI-VOA.

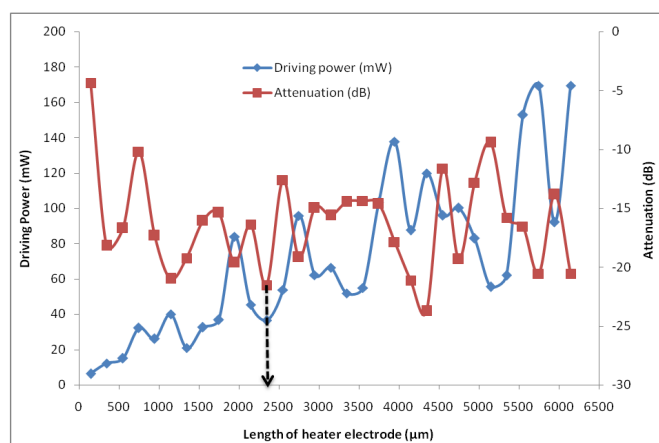


Figure 10. Simulated driving power and optical attenuation in the MMI VOA as a length function of the heater electrode.

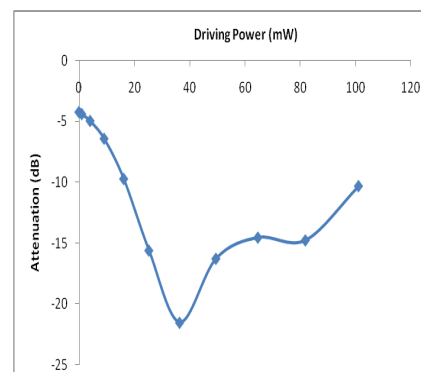


Figure 11. Attenuation characteristic for proposed MMI VOA with varied heater power (heater electrode length = 2347  $\mu\text{m}$ )

In comparison with other related works, Yang, *et al.* [28] and Jiang, *et al.* [29] have demonstrated the employment of VOA in enhancing the crosstalk performance of the optical switch. Work by Yang, *et al.* [28] on the digital optical switch (DOS) integrated with VOA reported a crosstalk value of -40 dB at applied power of 170 mW. Effort by Jiang, *et al.* [29] based on DOS with integrated S-bend VOA exhibited a crosstalk of -42 dB at an electrical power consumption of 140 mW. Although these works reported better crosstalk value, the electrical power consumed was much higher as compared to our proposed design. Hence, this comparison shows that our proposed integration of MMI switch and MMI-VOA is competitive in terms of crosstalk performance and switching power.

## 6. Conclusion

In this work, a variable optical attenuator has been successfully designed and characterized to improve a crosstalk performance in a polymer TO switch. The MMI platform has been adopted in device design. The MMI-TO switch has been realized with crosstalk of -19.14 dB and switching power of 54.41 mW. The proposed MMI VOA works well with low power consumption and attenuation level of 36.4 mW and -21.52 dB, respectively. It was observed that the total power consumption is 90.81 mW with improved crosstalk level of -36.37 dB. Significantly, the device integration has yield a crosstalk improvement up to 89.66%. In comparison with other published optical switch research, it was observed that our proposed device integration is competitive in terms of crosstalk performance and switching power.

## Acknowledgment

The authors wish to thank Universiti Teknologi Malaysia for funding this research work under Research University Grant Scheme.

## References

- [1]. Ke X, Wang MR and Li D. All-optical Controlled Variable Optical Attenuator using Photochromic Sol Gel Material. *IEEE Photonics Technology Letters*. 2006; 18: 1025-1027.
- [2]. Hurvitz T, Ruschin S, Brooks D, Hurvitz G and Arad E. Variable Optical Attenuator Based on Ion-Exchange Technology in Glass. *IEEE Journal of Lightwave Technology*. 2005; 23: 1918-1922.
- [3]. Qing F, Fang L, Chunxia W, Hongli X and Yuliang L. A Low Power Consumption Thermo-Optic Variable Optical Attenuator Based on Soi Material. 7<sup>th</sup> International Conference on Solid-State and Integrated Circuits Technology. 2004; 3: 2018-2020.
- [4]. Xia J, Yu J, Wang Z, Fan Z and Chen S. Low Power 2 x 2 Thermo-Optic Soi Waveguide Switch Fabricated by Anisotropy Chemical Etching. *Optics Communications*. 2004; 232: 223-228.
- [5]. Kim S, Hung YC, Geary K, Yuan W, Fetterman HR, Dinu DJR and Steier WH. Metal-defined

- Polymeric Variable Optical Attenuator. *Electronics Letters*. 2006; 18: 1055-1057.
- [6]. Sang-Shin L, Yong-Sung J and Yung-Sung S. Variable Optical Attenuator Based on a Cut off Modulator with Tapered Waveguides in Polymers. *IEEE Journal of Lightwave Technology*. 1999; 17: 2556-2561.
- [7]. May-Arrijoja DA, Selvas-Aguilar RJ, Escobedo-Alatorre P, LikamWa P, and Mondragon JJS. *Variable Optical Attenuator Using Active Multimode Interference Waveguide*. Proceedings of SPIE - The International Society for Optical Engineering. 2004; 5622: 731-734.
- [8]. Jiang X, Li X, Zhou H, Yang J, Wang M, Wu Y and Ishikawa S. Compact Variable Optical Attenuator Based on Multimode Interference Coupler. *Optics Communications*. 2005; 17: 2361-2363.
- [9]. He Y, Yang L, Fang Q, Xin H, Li F and Liu Y. Influence of Thermal Isolating Grooves on the Performance of the Mach-Zehnder Interferometer-Type Thermo-Optic Variable Optical Attenuator. *Optical Engineering Letters*. 2005. 44: 1-2.
- [10]. Noh Y-O, Lee C-H, Kim J-M, Hwang W-Y, Won Y-H, Lee H-J, Han S-G and Oh M-C. Polymer Waveguide Variable Optical Attenuator and its Reliability. *Optics Communications*. 2004; 242: 533-540.
- [11]. Yang L, Yu Y, Li F, Cheng Y, Qiu H and Wang Q. Simulations and Fabrication of Thermo-Optic Variable Optical Attenuators Based on Multimode Interference Coupler. *International Journal of Modern Physics B*. 2004; 16: 4275-4278.
- [12]. Diemeer MJB. Polymeric Thermo-Optic Space Switches for Optical Communications. *Optical Materials*. 1998; 9: 192-200.
- [13]. Louay Eldada. Polymer Integrated Optics: Promise vs. Practicality. DuPont Photonics Publications. 2002.
- [14]. Louay Eldada and L. W. Shacklette. Advances in Polymer Integrated Optics. *IEEE Journal of Selected Topics in Quantum Electronics*. 2000; 6: 54-68.
- [15]. Ibrahim MH, Lee S-Y, Chin M-K, Kassim NM and Mohammad AB. Multimode Interference Optical Splitter Based on Photodefinable Benzocyclobutene (BCB 4024-40) Polymer. *Optical Engineering*. 2007; 46: 013401-013404.
- [16]. Ibrahim MH, Kassim NM, Mohammad AB, Lee S-Y and Chin M-K. A Novel 1 × 2 Multimode Interference Optical Wavelength Filter Based on Photodefinable Benzocyclobutene (BCB 4024-40) Polymer. *Microwave and Optical Technology Letters*. 2007; 49: 1024-1028.
- [17]. Ibrahim MH, Lee S-Y, Chin M-K, Kassim NM and Mohammad AB. Multimode interference wavelength multi/demultiplexer for 1310 and 1550 nm operation based on BCB 4024-40 photodefinable polymer. *Optics Communications*. 2007; 273: 383-388.
- [18]. Bryngdahl O. Image formation using self-imaging technique. *Journal of the Optical Society of America*. 1973; 63: 416-419.
- [19]. Ulrich R and Ankele G. Self-imaging in Homogeneous Planar Optical Waveguides. *Applied Physics Letters*. 1975. 27; 337-339.
- [20]. Soldano LB and Penning MC. Optical Multi-Mode Interference Devices Based on Self-Imaging: Principle and Application. *IEEE Journal of Lightwave Technology*. 1995; 13: 615-627.
- [21]. The Dow Chemical Company. Product Literature: Cyclotene™ Advanced Electronic Resins. 1999.
- [22]. Mohd Haniff Ibrahim. Polymer Based Multimode Interference Optical Devices. PhD Thesis. Malaysia Universiti Teknologi Malaysia; 2007.
- [23]. Wang W-K, Lee HJ and Anthony PJ. Planar Silica-Glass Optical Waveguides with Thermally Induced Lateral Mode Confinement. *IEEE Journal of Lightwave Technology*. 1996; 14: 429-436.
- [24]. A.S.M. Supa'at. Design and Fabrication of a Polymer Based Directional Coupler Thermo-optic Switch. PhD Thesis. Malaysia: Universiti Teknologi Malaysia; 2004.
- [25]. Yaacob M, Ibrahim MH, Kassim NM, Mohammad AB and Supa'at ASM. Switching Power Improvement of Hybrid Polymer-Silica Based MMI Thermo-Optical Switch. *Journal of Optoelectronics and Advanced Materials*. 2009; 11: 559-564.
- [26]. Papadimitriou GI, Papazoglou C and Pomportsis AS. *Optical Switching*, Wiley-Interscience. 2007.
- [27]. Samdin N. Multimode Interference Structure for Thermo Optic Switch and Variable Optical Attenuator. Master in Electrical Engineering Thesis. Malaysia: Universiti Teknologi Malaysia; 2011.
- [28]. Yang M-S, Noh YO, Won YH and Hwang W-Y. Very Low Crosstalk 1x2 Digital Optical Switch Integrated with Variable Optical Attenuators. *Electronics Letters*. 2001; 37: 587-588.
- [29]. Jiang X, Qi W, Zhang H, Tang Y, Hao Y, Yang J and Wang M. Low Crosstalk 1 × 2 Thermo-optic Digital Optical Switch with Integrated S-Bend Attenuator. *IEEE Photonics Technology Letters*. 2006; 18: 610-612.